MODELLING ACOUSTIC TRANSMISSION LOSS DUE TO SEA ICE COVER

Polly Alexander[1,2], Alec Duncan[3], Neil Bose[1] and Daniel Smith[2]

[1]**Australian Maritime College, University of Tasmania, Maritime Way, Launceston, TAS 7248, Australia**
[2]**Intelligent Sensing and Systems Laboratory, CSIRO ICT Centre, Hobart, TAS, 7000, Australia**
[3]**CMST Curtin University, Kent Street, Bentley, Perth, WA, 6102, Australia**
pollyalexander@gmail.com

The propagation of underwater acoustic signals in polar regions is dominated by an upward refracting sound speed environment and the presence of a dynamic highly variable ice canopy. This paper provides an overview of the acoustic properties of sea ice and assesses the influence of ice canopy and water column properties on acoustic transmission loss for propagation within 20 km of a sound source at 20 m depth. The influence of the ice canopy is assessed first as a perfectly flat surface, and then as a statistically rough surface. A Monte Carlo method is used for the inclusion of ice deformation and roughness. This involves the creation of sets of synthetic ice profiles based on a given sea ice thickness distribution, followed by statistical methods for combining the output of individually evaluated ice realisations. The experimental situation being considered in the framing of this problem is that of an Autonomous Underwater Vehicle (AUV) operating within 50 m of the surface. This scenario is associated with a frequency band of interest of 9-12 kHz and a horizontal range of interest up to 20 km. The situation has been evaluated for a set of typical ice statistics using Ray and Beam acoustic propagation techniques. The sound speed profile (based on real data) results in a strong defocussing of direct path signals at ranges from 9-20 km and depths shallower than 50 m. This reduction in the signal strength of the direct path creates areas where the influence of surface reflected paths becomes significant. The inclusion of a perfectly flat ice layer reduces the transmission loss between 9-20 km by 15-50 dB. When the ice layer is included as a rough surface layer the results show a boost to signal strength of up to 8 dB in the small areas of maximum defocussing. Sea ice is a strongly time and space varying sea surface and exists in areas where defocussing of the direct path due to the sound speed profile reduces the range of direct path dominated transmission. This work presents methods for including a statistically relevant rough surface through a technique for generation of sets of surfaces based on ice deformation statistics. It outlines methods for including ice in acoustic modelling tools and demonstrates the influence of one set of ice statistics on transmission loss.

INTRODUCTION

Accurate sea ice volumes and under ice biology measurements are important inputs to global ocean climate and ecosystem models, and key indicators to monitor for change. With a heightened focus on climate science and change there is an increasing importance in measuring and monitoring what is happening under the ice covered oceans of the Arctic and Antarctic [1]. With advances in Autonomous Underwater Vehicle (AUV) capability the use of this technology in the ice environment is becoming more frequent [2–4]. AUVs operating in an open ocean environment use underwater acoustic communication for non safety-critical information and rely on their ability to surface and establish radio or satellite communication for critical situations such as navigation error or mission failure. In an under ice environment there is a far greater reliance on underwater communication as surfacing is no longer an option. Understanding and modelling acoustic propagation in an under ice environment is a key component in increasing safety and reliability in these deployments.

Typical Sound Speed Profiles (SSPs) in the Arctic and Antarctic produce an upward refracting sound environment, creating a sound channel that is continuously reflecting off the top ocean boundary, usually an ice layer. Variations in the top few hundred metres of the sound speed profile can create a defocussing of the direct path signal at ranges of 9-20 km. This defocussing creates a situation where the surface reflected paths provide a greater contribution to the received signal than would otherwise be experienced at such short ranges. To model propagation in this environment requires both the ability to create a realistic model of ice and the capability to incorporate the ice model within a framework for predicting acoustic propagation and transmission loss. The ice layer in a sea ice environment is a complex system made up of different ice types, ice thicknesses, roughness, and areas of ice deformation and ridging [5, 6]. This ice covered environment is highly variable with location, season and weather conditions. The presence of this spatially and temporally changing ice layer creates a large variation in the reliability of acoustic propagation.

There are two main parts to including an ice layer in an acoustic model. The first is consideration of the material properties of the ice layer in order to include the ice as an acoustic medium, and the second is the inclusion of randomly shaped and sized perturbations caused by sea ice ridging. Once the ice is included in the acoustic model there is then the question of what propagation modelling technique is most appropriate. There are five main techniques used in modelling underwater acoustic propagation. Ray theory, Normal Mode, Multipath Expansion, Wavenumber Integration (WI) or fast

field, and Parabolic Equation (PE) [7]. Etter [7] reviews and summarises modelling and simulation techniques reported up to 2001. For higher frequency work ray tracing provides the fastest solution with a minor compromise in accuracy [8]. The Acoustics Toolbox [9] is an open source modelling tool that provides a selection of environment and propagation modelling tools within the one software framework. The BELLHOP program is a Fortran ray and beam forming code that is part of the Acoustics Toolbox [9].

This paper reviews these two main parts of including an ice layer and investigates and reports on a method for including a variably ridged layer. Techniques for creating simulated ice cover from sea ice statistics are discussed and a case study involving a typical set of ice statistics is evaluated using BELLHOP. This work considers the influence of including an ice layer in short range acoustic modelling and compares direct path results with flat ice and the results of the presented technique for including statistically rough ice, for a frequency of 10 kHz a range of 20 km and receiver depths shallower than 50 m. Ray tracing is used as the most computationally feasible propagation model for this frequency and range scenario.

Background

There has been significant research into under ice sound propagation in the Arctic since the 1960s. This is due to the disputed nature of borders in this area, defence prerogatives, the potential for natural resources, and the capability for long range propagation. The consequence of this is a body of research investigating the influence of an ice canopy on acoustic propagation at both low and high frequencies. Low frequencies have the potential for long range propagation, whereas high frequency signals undergo greater scattering and attenuation losses both in the sea water and due to the roughness dimensions of the ice and the frequency dependence of its attenuation [10–12]. For high frequencies (>15 kHz) the report by the Applied Physics Laboratory, University of Washington [13] provides a comprehensive section on acoustics in the Arctic. For low frequency there are many investigations into long range propagation that examine low frequency interaction with ice [10, 11, 14].

Compared to many of the long range propagation scenarios considered in the Arctic, communication systems for AUV deployment require relatively high frequencies (9-12 kHz) and short ranges (<100 km). Typical underwater acoustic modems operate between 8-13 kHz, with some modems reporting frequency ranges of 3-30 kHz [15].

SEA ICE

The formation of sea ice is dictated by the weather (meteorological) and water (hydrographical) conditions at the time of formation and through its life cycle. These conditions control the temperature, salinity, density and crystal structure of the ice as it is formed, and as the ice grows in thickness the different layers tell the story of the conditions under which it was created [16]. A large amount of sea ice is formed and decays within a single winter, summer cycle and is referred to as first year ice. In a typical growth scenario, sea ice first forms as slush from the collection of ice crystals in open water. It then consolidates into small distinct plates, or pancake ice, these combine to make larger floes that are further influenced by environmental conditions and deformed to create a ridged ice environment. This process means that sea ice is a range and time varying surface layer, in both thickness, roughness and material properties.

Jezek et al. [17] describe the impact on the acoustic properties of sea ice due to the change in surface texture at different growth stages. They separate this into three states: slush, growing, and consolidated ice. The growing stage involves the formation of pure ice dendrites, a crystal that forms with a tree like form [18], that acts as a skeletal layer on the ice surface collecting salty brine pockets. Consolidated ice is where the ice has formed a solid bottom surface and the slush stage is where there is only slush ice on the surface. Throughout these stages of growth the ice becomes a better acoustic reflector with slush ice attenuating a signal ten times more than growing ice which itself attenuates a signal five times more than consolidated ice (reported for high frequency near normal incidence) [17, 19].

The two main methods of mechanical ice thickening are ridging and rafting of ice floes. Sea ice ridging is formed by the shearing and compression of ice floes pressing out ice blocks below and on the surface of the ice [20]. Rafting of ice is where one ice floe is pushed on top of another pushing the bottom floe into the water. Shear ridging creates small chunks of ice with a ground up appearance while both pressure ridging and rafting create a collection of more discrete blocks of different shapes, sizes and orientations [13]. These mechanical forces create features, with the air-ice surface features referred to as sails, and the ice-water surface features referred to as ice keels. These forces are not symmetric and the ridge sails undergo significantly different weathering than keels. While this weathering is not symmetric there is correlation between top and bottom geometries that can be used to estimate bottom roughness from surface features [11, 21]. As sea ice undergoes its many deformations the underside becomes a continuously rough surface in which the exact definition of any distinctive feature, as opposed to the other roughness of the surface, varies [22].

Material properties of sea ice

As ice supports both shear and compressional acoustic propagation it can be modelled as an elastic medium. The temperature and salinity profiles of an ice layer control the density and the porosity of the ice which then dictates the elastic properties and the reflection loss of acoustic waves interacting with the ice [13, 23]. Ice porosity and ice sheet thickness are reported to have the largest influence on the acoustic properties of the ice [24] with salinity and temperature variation within the ice having less effect [12]. If the shear velocity is less than the speed of sound in water, a vertically polarised shear velocity, as reported by Kuperman and Schmidt [25] occurs, at which point the air-ice boundary also becomes significant to the model. Hunkins [26] measured and analysed shear and compressional waves within an ice sheet. The shear waves are understood to interfere with compressional waves and the acoustic field in the water close to the ice boundary [8, p443]. McCammon and

McDaniel show that the elastic properties of the ice play an important role in attenuation of a plane wave on an ice surface at both high and low frequencies [12].

A more complex ice model is used by McCammon and McDaniel [12] who model ice as a multi-layered elastic solid bounded on both sides by a fluid half space, and Yew [24] who models it as a 'transversely isotropic brine saturated porous medium'. Modelling ice as a multi-layered medium allows for the inclusion of a skeletal growth layer and surface snow as well as variability with the ice itself. The acoustical properties to describe an ice layer can either be found through specific experiments to measure the sound velocities in the ice or through processing of temperature and salinity measurements.

A method for calculation of the acoustic parameters from temperature and salinity is summarized in the report by the Applied Physics Laboratory [13]. It summarises the process of calculating density and porosity from temperature and salinity then provides equations to compute compressional speed, shear speed and bulk moduli, and gives an approximation for attenuation as a function of frequency and temperature [12].

An ideal model to include the material properties of sea ice could take as input the properties of the ice and supply information to a propagation model such that it can calculate reflection effects. An appropriate description of ice for a model could consists of a combination of the following:

- the acoustic properties of the ice: ice density (ρ), compressional wave speed and attenuation (C_p, A_p), shear wave speed and attenuation (C_s, A_s)
- the physical properties of the ice: temperature, salinity, air/ice temperature, ice growth stage
- the morphological properties of the ice: thickness, ice-water roughness, ice-air roughness, ridging statistics

from which a model would calculate or estimate the reflection losses and phase change with incident angle.

Sea ice as a rough surface

As sea ice undergoes many deformations the underside becomes a continuously rough surface. A view of this roughness in the Antarctic sea ice pack taken by a Remotely Operated Vehicle (ROV) is show in Fig. 1 to illustrate some of the shapes that are possible. Sea ice thickness is often described using a histogram of an ice thicknesses descriptor over the area being considered [5, 27]. Depending on the scale of roughness being investigated descriptors used for variation in the ice surface are: thickness; draft; and keel size. Ice draft is the measurement of ice depth/thickness measured from the water freeboard. Ice feature count and thickness histograms form amplitude distribution functions for a discrete area of sea ice, and can be described by a Probability Density Function (PDF) and spatial power spectrum.

Sea ice density and rafting impacts are such that sea ice is much deeper below the surface than it is tall above the surface which results in an asymmetric thickness PDF with a long positive tail. This is even more the case when considering the PDF of ice draft with the freeboard an upper limit in one direction and the potential for deep keel features creating large extremes in ice draft depth. Depending on the ice environment the thickness/draft PDF may also contain multiple peaks representative of different ice types, areas of different mean thickness, or age within the one profile [28].

Figure 1. View of Antarctic sea ice from below taken by a ROV. This picture illustrates the roughness of the surface. Photo courtesy of the Australian Antarctic Division ROV team

One way of describing the roughness from this information is by characterising the shape of the histogram and fitting it to a known distribution. Previous work characterising the distribution of the sea ice features has not provided a single solution with Gaussian, Gamma, Poisson, Rayleigh, a combination of multiple log normals, and power spectrum descriptions being suggested.

Simulated sea ice

Simulation of ice profiles based on measured or predicted sea ice statistics allows the translation of ice thickness or roughness statistics to acoustic propagation and transmission loss statistics. This translation can be achieved through Monte Carlo simulation or generation of larger, keel feature statistics, such as that suggested by Diachok [21]. Simulation from ice statistics also creates an interface for using output from global climate models that include representations of sea ice for given locations and times to predict an acoustic environment that has not been sampled.

There are two techniques in the literature for creating simulated sea ice draft profiles. The first provided by Hughes [28], uses a combination of log-normal distributions to describe and generate ice profiles. The second proposed by Goff [29] using a covariance model and a gamma based PDF description.

Goff [29] describes the sea ice draft distribution using the following descriptors:

- Mean ice draft t_0
- Normalised skewness μ_3^n
- Characteristic length λ_θ
- RMS variation H
- Fractal dimension D

Hughes [28] specifies the sea ice draft as a combination of seven log-normal curves each described by:

- Individual contribution to the total PDF
- Mean of the log of the individual peak
- Standard deviation of the individual peak

Hughes provides a more complex description of the ice amplitude distribution by including different peaks for different ice types within the one sample area. The multi modal representation of this technique would give it a strong advantage if the ice region being considered covered areas of distinctly different ice types. It reports a very accurate fit to reported ice draft data from different experimental data sets.

Goff's technique provides an approximation of the ice draft amplitude variability as a gamma PDF. The Gamma PDF provides a good model of the asymmetric, long tailed nature of the ice draft measurements, but only includes one peak. The use of a single, standard PDF for ice draft makes this approach easier to implement, but less robust to areas of different ice types, compared with the multi peaked approximation of Hughes.

METHODS

A test case has been implemented to demonstrate this method for including simulated rough ice in the Acoustics Toolbox and to evaluate the influence of including ice on transmission loss for one scenario.

The roughness and depth of each ice realisation was included using an altimetry file that specified the depth of the water ice boundary with range. The Goff method for ice simulation was implemented to create a set of altimetry files for a set of ice descriptors. Goff's technique is selected to evaluate the difference between including a single ice type and including flat ice. Two of the sets of ice statistics described in Goff [29] are shown in Table 1 to show the variation in statistics with ice type. Figure 2 shows simulated ice profiles for these two sets of ice statistics paired with normalized histograms of the deviation from the mean draft. This shows the large amount of surface roughness generated by this technique, the conformity of the simulated profile to the gamma distributions they are based on and the variability between two different sets of ice descriptive statistics. Three instances of each ice statistic are displayed to show the variability within this random sampling. The ice statistics from the first line of this table describing the what is refereed to as 'typical' ice conditions are used in this case study. The generated profiles were processed into altimetry files with 1 m horizontal resolution, that were then entered into the Acoustics Toolbox environment specification and used in the calculation of ray path and transmission loss by BELLHOP. For this typical ice case 25 synthetic ice profiles of 20 km length were created using the Goff technique described in the *Simulated sea ice* section.

The acoustic properties of the ice were included through the specification of a reflection coefficient file that provided a look up table of reflection amplitude and phase change as a function of incidence angle. For this case study the ice layer was modelled as an air backed layer using the acoustic properties of ice approximated by Jensen et al. [8] as: compressional speed 3500 m/s; shear speed 1800 m/s; density 890 kg/m^3; compressional attenuation 0.4 dB/λ_p; and sheer attenuation 1.0 dB/λ_s and a thickness of 2.7 m corresponding to the mean ice draft of the typical ice conditions described by Goff. These two layers were specified as input to the *bounce* program, that is part of the Acoustics Toolbox, which computes the

Table 1. Ice morphology statistics from test cases presented in Goff [29]. Ice is described by mean ice draft (t_0), normalised skewness (μ_3^n), characteristic length (λ_θ), RMS variation (H), and fractal dimension (D)

	t_0 [m]	μ_3^n	λ_θ[m]	H [m]	D
Typical Ice					
1	2.76	1.81	40.5	1.38	1.37
Large RMS variation and Low Skewness					
2	4.52	1.27	63.8	3.84	1.26

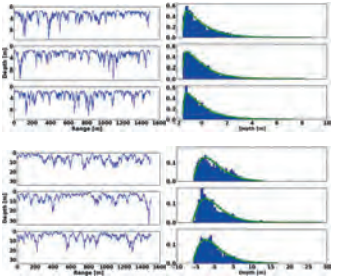

Figure 2. A random selection of simulated ice drafts with histograms of deviation from mean ice thickness and the probability density functions they are based on. Ice statistics used are those described in Goff [29] and are shown in Table 1. The top figure is based on what are identified as typical ice conditions in the field location reported by Goff and the bottom is for an ice type identified as an area of large RMS and low skewness ice

combined reflection coefficient for a stack of media for a given frequency. The reflection coefficient for 10 kHz generated using this technique is shown in Fig. 3.

The Acoustics Toolbox environment was set up with input parameters shown in Table 2. The Sound Speed Profile (SSP) used was based on the down cast of a Conductivity Temperature Depth (CTD) cast taken in Antarctica on November 22nd 2010 at Latitude 64°35 South, Longitude 81°57 East. The data from the CTD cast were combined using the formula presented by Medwin [30] for sound speed shown in Eq. (1) where T is temperature in °C, S is salinity in practical salinity units (p.s.u.), and z is water depth in metres.

$$C(T,S,z) = 1449.2 + 4.6T - 0.055T^2 + 0.00029T^3 + (1.34 - 0.010T)(S-35) + 0.016z \quad (1)$$

For the cast depth of 600 m used here this formula provides sufficient accuracy [31]. The calculated sound speed for the full cast with the raw temperature and salinity data is shown in Fig. 4. In the case study only the down cast was used and the SSP was extrapolated to the full 2 km depth assuming

minimal change in salinity and temperature beyond the depth of the cast.

Monte Carlo methods work on the principle of combining the output of many instances, randomly sampled from an input distribution, to produce an output representative of the input space. In this case, simulated ice draft profiles are created using a statistical distribution of the ice. The acoustic field is calculated individually for each simulated draft and the combined outputs provides a statistical representation of the acoustic field for that ice sample space. BELLHOP was run individually for each simulated profile to produce an incoherent pressure field p_i. These fields were then combined as an incoherent average as described in Eq. (2).

$$p_{RMS} = \sqrt{\frac{\sum_{i=0}^{N} |p_i|^2}{N}} \tag{2}$$

The average transmission loss was then calculated using Eq. (3).

$$TL_{avg} = -20\log_{10}(p_{RMS}) \tag{3}$$

Two reference case incoherent pressure fields were also calculated. The first, p_{dp}, including the direct path only by removing beams on surface interaction, and the second, p_{flat}, using a flat ice case with an ice boundary at a constant 2.7 m. The differences diagrams in the results section are evaluated as a difference between two fields in decibels using Eq. (4).

$$Rel = 20\log_{10}\left(\frac{p_1}{p_2}\right) \tag{4}$$

RESULTS AND DISCUSSION

The increase in sound speed with depth evident in Fig. 4 results in sound being refracted upwards towards the sea surface. However, the marked departure of the profile from a straight line results in this refraction being non-uniform, producing strong focusing of sound at some ranges and defocussing at others. In particular there is strong defocussing near the sea surface at ranges between nine and twenty kilometres. This result can be seen in the direct-path only transmission loss and ray trace plots shown in Fig. 5.

The inclusion of a flat ice layer using the method specified above produces a consistent acoustic field with much lower transmission loss beyond 9 km than if only the direct path is included. The transmission loss and ray tracing results for the flat ice case are shown in Fig. 6. The transmission loss for the flat ice case is similar to what would be expected for an open water surface. This can be explained by evaluating the grazing angles of the rays that are interacting with the surface as shown in Fig. 7. This figure shows that almost all the surface interactions take place with a grazing angle less than 10 °. Figure 3, showing the reflection coefficient for an air-backed layer of ice 2.7 m thick at 10 kHz, shows only minimal reduction in the magnitude of the reflection coefficient for these small angles, explaining the near open water result.

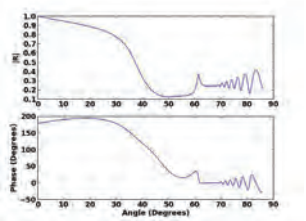

Figure 3. Reflection coefficient for combined medium: water, 2.7 m of ice, air at 10 kHz

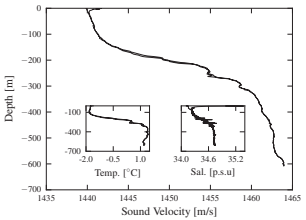

Figure 4. Sound speed profile measured in the Antarctic Ocean with temperature and salinity shown as inset figures. Values from the down cast were extrapolated to the 2 km depth for use in the case study presented in this paper

Table 2. BELLHOP Inputs

Parameter	Value
Environment	
Frequency	10 kHz
Range	20 km
Environment depth	2.0 km
Transmission loss	Incoherent
Bottom surface	Water matched
Source	
Source depth	20 m
Beam type	Gaussian
Start Angle (from horizontal)	-20 °
End Angle (from horizontal)	20 °
No. beams	10,000
Receivers	
Number horizontal	200
Number vertical	100
Max receiver depth	50 m
Max receiver range	20 km

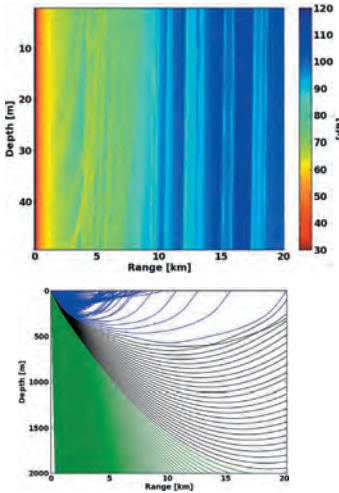

Figure 5. Direct Path only transmission loss for the top 50 m of interest and a ray trace for the full 2 km depth. Red rays touch top and bottom surfaces, green bottom only, blue surface only and black neither surface

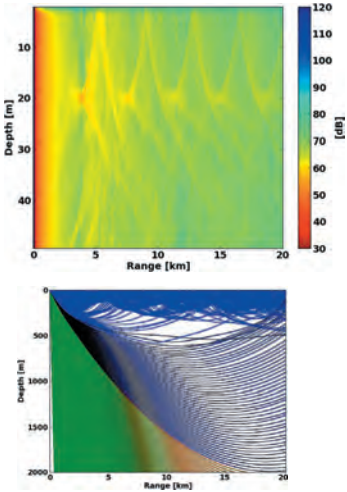

Figure 6. Transmission loss and ray trace for a flat ice surface. The flat ice surface uses compressional speed 3500 m/s; shear speed 1800 m/s; density 890 kg/m^3; compressional attenuation 0.4 dB/λ_p; and sheer attenuation 1.0 dB/λ_s and a thickness of 2.7 m corresponding to the mean ice draft thickness. Red rays touch top and bottom surfaces, green bottom only, blue surface only and black neither surface

The difference between the direct path only and the inclusion of a flat ice layer can be seen in Fig. 8 which shows the difference as calculated by Eq. (4) with p_1 being the flat ice pressure field and p_2 being the direct path only pressure field. This difference representation highlights the defocussing of the direct path only transmission loss and suggests that in the presence of flat ice the received signal strength would be much higher than if considering only the sound that reaches the receiver without interacting with any boundaries.

Results calculated using the Monte Carlo method for the case of deformed sea ice show significantly less surface reflected contribution. The results of the averaged pressure field from the Monte Carlo simulation are shown in Fig. 9. This result shows some filling in of the defocussed band at 17 km but the difference is only 8 dB, as opposed to 42 dB for the flat ice case.

The difference between this rough ice surface realisation and the direct path as calculated by Eq. (4) with p_1 being the ridged ice pressure field and p_2 being the direct path only pressure field is shown in Fig. 10. The reason for this reduction of the signal with the inclusion of the rough surface is clearly seen in Fig. 11 which shows the ray trace for a single rough ice instance with increasing scale. This figure illustrates the majority of surface interacting rays being reflected down or back rather than along a forward propagating path as was the case with the flat ice scenario.

Approximations and assumptions

The acoustic parameters and ice roughness statistics used in the test case were approximations from the literature. As discussed in sections *Material properties of sea ice* and *Sea ice as a rough surface* it would be more realistic to calculate these values for the expected temperature, salinity, density, thickness and deformation statistics for the area being evaluated. These can be predicted from global climate models or are available in data sets from previous field studies.

In the Antarctic or Arctic sea ice pack there is unlikely to be 20 km ice surfaces of the one ice type. This single ice type test case is provided to show the impact of being able to include both flat and rough ice in acoustic transmission estimates. Future work could involve a more realistic combination

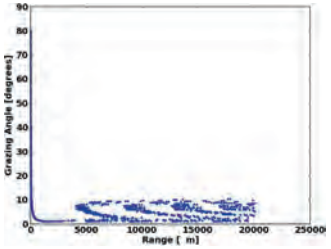

Figure 7. Grazing angles for rays interacting with the flat ice surface

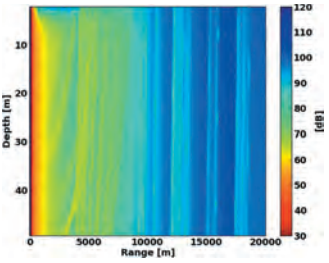

Figure 9. Monte carlo rough surface average transmission loss

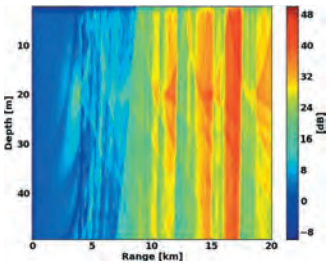

Figure 8. Difference in decibels between the estimated received fields when representing the surface as a flat ice sheet and direct path only. The difference is calculated by Eq. (4) with p_1 being the flat ice pressure field and p_2 being the direct path only pressure field

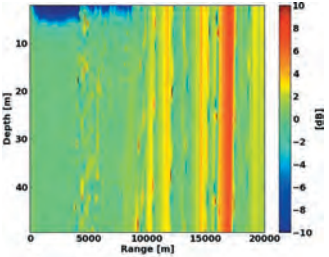

Figure 10. Difference in decibels between representing the surface as a rough ice canopy and direct path only

of different ice types in anticipated autonomous vehicle deployment areas. The location of the source relative to flat ice, open water, or rough ice could have a large influence on the range of effective signal detection.

This treatment of sea ice is only considering it as a two dimensional profile while real sea ice has a third dimension. Future work could compare the validity of this two dimensional approximation and assess the requirement for full three dimensional modelling.

The case study shown uses a simplification of the reflection coefficient based on a single ice thickness. This assumes the top side of the ice is exactly following the bottom surface of the ice to maintain a uniform width, which is not a physically realistic assumption. To assess this assumption the reflection coefficient was calculated at 10 kHz for a range of different ice thicknesses and the results of this are shown in Fig. 12. As can be seen in Fig. 12 for ice thicknesses over 0.3 m there is little change in the magnitude of the reflection coefficient with ice thickness for grazing angles up to 35 °. What is missing from this reflection coefficient is the consideration of the influence of having a snow or water backed layer, which could be added in a more complex simulation.

The case study does not consider the signal returned by bottom reflection but this could easily be included if the scenario demanded it.

A limitation of using ray tracing is that scattering angles depend solely on the local ice slope and diffraction effects are ignored. It is therefore only considered valid at roughness scales (both horizontal and vertical) much larger than the acoustic wavelength. For a 10 kHz signal in a 1440 m/s water sound speed the wavelength is 14 cm. Future work could involve the division of the ice roughness into wavelength relative large and small features. The influence of smaller features could be included using the Rayleigh roughness parameter and larger scale features included using the altimetry file as detailed here.

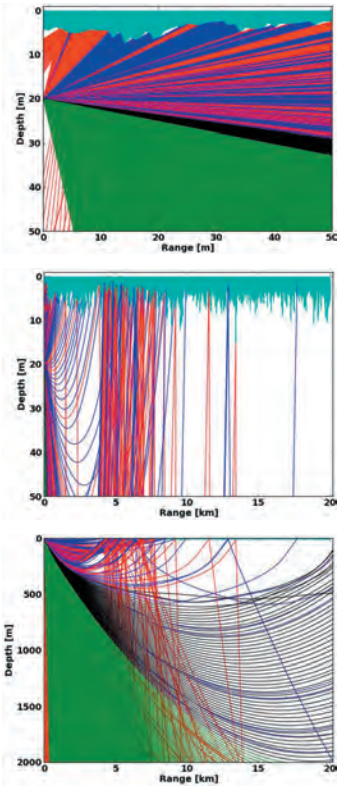

Figure 11. Ray traces for a single instance of a rough canopy shown at three different scales. The three scales are given to provide a complete picture of the rays interacting with the ice surface. Red rays touch top and bottom surfaces, green bottom only, blue surface only and black neither surface

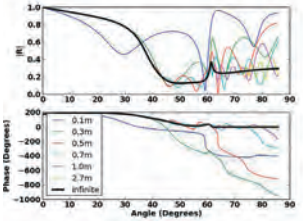

Figure 12. Reflection coefficient at 10 kHz for combined medium: water, ice, air with varying ice thickness

CONCLUSIONS

This paper presents a method, referred to as the Monte Carlo Method, for generating acoustic field information based on a set of simulated ice draft profiles. This has been done with the aim of providing a detailed prediction of an under ice sound environment to support autonomous vehicle deployment reliant on acoustic communications.

It was found that certain polar sound speed profiles, such as the one presented in this case study, create a strong defocussing in the direct path. While it might be expected that surface reflection would have little influence at these shorter, 20 km ranges, this reduction in the strength of the direct path creates a situation where the surface reflected paths dominate the total acoustic field.

Inclusion of a rough sea surface using the Monte Carlo method greatly reduced the contribution of ice surface reflected paths. There was a slight increase of approximately 8 dB over the direct path only case in the defocussed areas, but overall the transmission loss estimate for rough ice was closer to the direct path only case than the flat ice surface case.

If the simulated ice profiles are considered representative of the ice in a given region and season then the Monte Carlo method provides a representative estimation of the acoustic field based on situations that could be encountered. The statistical nature of this approach provides a tool for risk management for autonomous vehicle deployment where worst, best and mean cases for signal propagation could be evaluated. By including the simulated ice profiles directly the Monte Carlo approach can be used with different methods of generating simulated ice. This allows acoustic simulation in ice areas to use all the information available about the expected ice conditions when predicting transmission loss, expected signal range and risk areas.

In real sea ice conditions the surface consists of patches of heavily deformed ice, gently sloping rafted ice, growing ice, and open water. This work shows the significance of being able to include a model of the ice surface in acoustic transmission loss estimates and suggests further work considering more detailed and accurate measures for undertaking this inclusion.

REFERENCES

[1] P. Wadhams, "Sea ice", In J.H. Steel, K.K. Turekian and S. Thorpe, editors, *Encyclopedia of Ocean Sciences*, volume 1, chapter Sea Ice, pages 141–158. Academic Press, Oxford, 2nd edition, 2009

[2] P. Wadhams and M.J. Doble, "Digital terrain mapping of the underside of sea ice from a small AUV", *Geophysical Research Letters* **35**(1), 1–6 (2008)

[3] M. Jakuba, C. Roman, H. Singh, C. Murphy, C. Kunz, C. Willis and T. Sato, "Long-Baseline Acoustic Navigation for Under-Ice AUV Operations", *Journal of Field Robotics* **25**(11-12), 861–879 (2008)

[4] C. Kaminski, T. Crees and J. Ferguson, "12 days under ice an historic AUV deployment in the Canadian High Arctic", *Proceedings of Autonomous Underwater Vehicles*, pages 1–11, Monterey, CA, 2010

[5] A.P. Worby, C.A. Geiger, M.J. Paget, M.L. van Woert, S.F. Ackley and T.L. DeLiberty, "Thickness distribution of Antarctic sea ice", *Journal of Geophysical Research* **113**(C5), 1–14 (2008)

[6] N. Untersteiner, editor, *The Geophysics of Sea Ice*, Springer, New York, 1st edition, 1987

[7] P. Etter, "Recent advances in underwater acoustic modelling and simulation", *Journal of Sound and Vibration* **240**, 351–383 (2001)

[8] F.B. Jensen, W.A. Kuperman, M.B. Porter and H. Schmidt, *Computational ocean acoustics*, Springer, London, 2011

[9] M.B. Porter, Acoustic Toolbox, `http://oalib.hlsresearch.com/Modes/AcousticsToolbox/`

[10] H. Kutschale, "Arctic hydroacoustics", *Proceedings of the U.S. Naval Arctic Research Laboratory Dedication Symposium* **22**(3), 246–264 (1969)

[11] A.N. Gavrilov and P.N. Mikhalevsky, "Low-frequency acoustic propagation loss in the Arctic Ocean: Results of the Arctic climate observations using underwater sound experiment", *Journal of the Acoustical Society of America* **119**(6), 3694–3706 (2006)

[12] D. McCammon and S. McDaniel, "The influence of the physical properties of ice on reflectivity", *Journal of the Acoustical Society of America* **77**(2), 499–507 (1985)

[13] Applied Physics Laboratory, *APL-UW High-frequency ocean environmental acoustic models handbook*, Technical report, University of Washington, Seattle, Washington, 1994

[14] E.Y.T. Kuo, "Low-frequency acoustic wave-scattering phenomena under ice cover", *IEEE Journal of Oceanic Engineering* **15**(4), 361–372 (1990)

[15] L. Freitag, M. Grund and S. Singh, "The WHOI micro-modem: An acoustic communications and navigation system for multiple platforms", *IEEE Proceedings of Oceans 2005*, pages 1–7, Washington D.C, 2005

[16] H. Eicken, "From the microscopic, to the macroscopic, to the regional scale: growth, microstructure and properties of sea ice", In D.N. Thomas and G.S. Dieckmann, editors, *Sea Ice: An introduction to its Physics, Chemisty, Biology and Geology*, chapter 2. Wiley-Blackwell, 2003

[17] K.C. Jezek, T.K. Stanton and A.J. Gow, "Influence of environmental conditions on acoustical properties of sea ice", *Journal of the Acoustical Society of America* **88**, 1903–1912 (1990)

[18] T.K. Stanton, "Acoustical reflection and scattering from the underside of laboratory grown sea ice: Measurements and predictions", *Journal of the Acoustical Society of America* **80**(5), 1486–1494 (1986)

[19] G.R. Garrison, "Acoustic reflections from arctic ice at 15-300 kHz", *Journal of the Acoustical Society of America* **90**(2), 973–984 (1991)

[20] A. Marchenko and A. Makshtas, "A dynamic model of ice ridge buildup", *Cold Regions Science and Technology* **41**(3), 175–188 (2005)

[21] O.I. Diachok, "Effects of sea-ice ridges on sound propagation in the Arctic Ocean", *Journal of the Acoustical Society of America* **59**(5), 1110–1120 (1976)

[22] D. Rothrock and S. Thorndike, "Geometric properties of the underside of sea ice", *Journal of Geophysical Research* **85**(C7), 3955–3963 (1980)

[23] S.D. Rajan, "Determination of compressional wave and shear wave speed profiles in sea ice by crosshole tomography Theory and experiment", *Journal of the Acoustical Society of America* **93**(2), 721–738 (1993)

[24] C. Yew, "A study of reflection and refraction of waves at the interface of water and porous sea ice", *Journal of the Acoustical Society of America* **82**, 342–353 (1987)

[25] W.A. Kuperman and H. Schmidt, "Rough surface elastic wave scattering in a horizontally stratified ocean", *Journal of the Acoustical Society of America* **79**, 1767–1777 (1986)

[26] K. Hunkins, "Seismic studies of sea ice", *Journal of Geophysical Research* **65**(10), 3459–3472 (1960)

[27] R.H. Bourke and R.P. Garrett, "Sea ice thickness distribution in the Arctic ocean", *Cold Regions Science and Technology* **13**, 259–280 (1987)

[28] B.A. Hughes, "On the use of lognormal statistics to simulate one-and two-dimensional under-ice draft profiles", *Journal of Geophysical Research* **96**, 101–111 (1991)

[29] J.A. Goff, "Quantitative analysis of sea ice draft, 1, Methods for stochastic modeling", *Journal of Geophysical Research Oceans* **100**, 6993–7004 (1995)

[30] H. Medwin, "Speed of sound in water: A simple equation for realistic parameters", *Journal of the Acoustical Society of America* **58**(6), 1318–1319 (1975)

[31] X. Lurton, *An Introduction to Underwater Acoustics: Principles and Applications*, Springer, Chichester, UK, 2002